

Thianthrene Radical Cation Hexafluorophosphate

Johannes Beck^a, Thomas Bredow^b, and Rachmat Triandi Tjahjanto^a

^a Institute of Inorganic Chemistry, Bonn University, Gerhard-Domagk-Str. 1, 53121 Bonn, Germany

^b Institute for Physical and Theoretical Chemistry, Bonn University, Wegelerstr. 12, 53115 Bonn, Germany

Reprint requests to Prof. Dr. J. Beck. Fax: +49 (228) 73 5660. E-mail: j.beck@uni-bonn.de

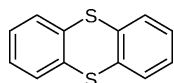
Z. Naturforsch. **2009**, 64b, 145 – 152; received September 16, 2008

In the presence of $[NBu_4][PF_6]$ as the electrolyte, thianthrene (TA) is transformed by electrochemical oxidation to thianthrenium hexafluorophosphate containing the $TA^{\bullet+}$ radical cation. The reactions were performed in CH_2Cl_2 , H_3CCN , and liquid SO_2 as solvents. In CH_2Cl_2 , $TA[PF_6]$ is sparingly soluble and is deposited directly in crystalline form on the platinum electrode. In H_3CCN and liquid SO_2 , $TA[PF_6]$ is highly soluble and gives dark blue solutions from which it can be crystallized upon concentration of the solutions. The air sensitive crystals are black with bronze metallic luster. They belong to the monoclinic system ($C2/m$, $a = 12.4345(8)$, $b = 10.5318(6)$, $c = 11.1303(7)$ Å, $\beta = 112.565(3)^\circ$) and are built up of almost planar $TA^{\bullet+}$ cations and octahedral $[PF_6]^-$ anions. The F atoms of the anions are disordered over two positions. The radical cations are associated to form dimeric units $(TA^{\bullet+})_2$ with the planar molecules stacked with two weak $S \cdots S$ bonds (3.06 Å). In the crystal these dimers are separated by the $[PF_6]^-$ anions. Electrical conductivity measurements show $TA[PF_6]$ to be a small-gap semiconductor. Conductivity is low at r.t. but reaches $2.5 \cdot 10^{-5}$ S m⁻¹ at 110 °C, the activation energy in the high-temperature region amounts to 1.2 eV. Periodic quantum-chemical calculations at hybrid density-functional level predict a strong coupling between neighboring $(TA^{\bullet+})$ spin centers, resulting in a singlet ground state. The calculated band gaps of both singlet (1.5 eV) and triplet (0.9 eV) states are small, consistent with the measured conductivity.

Key words: Thianthrene, Radical, Hexafluorophosphate, Conductivity, Band Structure, Crystal Structure

Introduction

For more than one hundred years the intensive color of solutions of thianthrene (TA) in sulfuric acid has been known which is caused by the oxidation of TA to the radical cation $TA^{\bullet+}$ under release of SO_2 [1]. The neutral molecule is non-planar and bent along the intramolecular $S \cdots S$ axis by 131° as determined by electron diffraction in the gas phase [2], and by 128° as determined by single crystal X-ray diffraction [3]. Several theoretical calculations were reported dealing with the molecular conformation in gas-phase and solution and its interpretation [4–8].



Molecular structure of thianthrene (TA).

Different ways for oxidation of TA to the radical cation have been reported. These include the reaction of TA with perchloric acid in hot acetic anhydride [9], the reaction of TA with its monoxide in nitromethane and perchloric acid or tetrafluoroboric acid [10], the

reaction of TA and ICl in carbon tetrachloride [11], the reaction of TA with $SbCl_5$ in chloroform [12], the reaction of TA with $NO[BF_4]$ in acetonitrile [13], and the reaction of TA with $AlCl_3$ in methylene chloride [14]. The structure determination of thianthrenium tetrachloroaluminate revealed the significant structural change caused by the oxidation. In contrast to the bent neutral molecule, the radical cation turned out to be almost planar [14]. This is interesting since the odd number of electrons does not meet Hückel's $4n + 2$ rule for an aromatic system. As found by the structure determination, the radical cations in $(TA^{\bullet+})[AlCl_4^-]$ form dimers in the crystal. This tendency to dimerize was already known from studies of solutions. By visible light absorption spectra and *in situ* ESR spectroscopy in solution the formation of dimers could be shown to be strongly dependent of the solvent [15], concentration and temperature [16].

The molecular arrangement of planar molecules in the crystalline state depends on many parameters and is in general hard to predict. Even such a long known

organic radical ion like thianthrenium can bring a surprise. The oxidation of TA with the dodecamethylboranyl radical yielded $(TA)_3(B_{11}(CCH_3)_{12})_2$ containing a thianthrene triple-decker $(TA)_3^{2+}$ carrying two positive charges with a unique tilted position of the middle molecule [17].

Liquid SO_2 had already turned out as a suitable solvent for redox processes involving aromatic heterocyclic molecules. Cyclic voltammetry at $-40\text{ }^{\circ}\text{C}$ in this solvent showed TA to undergo two oxidation steps leading to the monocation and to the dication [18]. These potentials are generally slightly solvent-dependent. In organic media differences of 10 mV for the first and 20 mV for the second oxidation step were observed [19]. To study the influence of the solvent we performed the syntheses by electrocrystallization both in frequently used organic solvents and in the rarely used liquid SO_2 . Since structural information of compounds containing unsubstituted TA radical ions is limited we concentrated our interest on the radical ion salt of TA with hexafluorophosphate as the anion.

Results and Discussion

Electrochemical synthesis and properties of $TA[PF_6]$

The electrochemical oxidation of thianthrene can be performed in different solvents. The salt-like compound $TA[PF_6]$ is only sparingly soluble in CH_2Cl_2 with the consequence that $TA[PF_6]$ formed during applying electrical current is deposited on the surface of the electrode. A polycrystalline layer is generated on the platinum wire which can be isolated in the glove box. In CH_3CN and liquid SO_2 $TA[PF_6]$ is well soluble. In these solvents the solution in the anodic part of the cell turns dark blue and even after prolonged electrolysis no deposition on the electrode or precipitation of solid material occurs. $TA[PF_6]$ was isolated by distilling off the solvent and, in the case of CH_3CN , allowing diethyl ether to diffuse into the concentrated solution. In the case of liquid SO_2 , the solvent was released as a gas at r.t., and after concentration to one third of the original volume black crystals of bronze metallic luster appeared on cooling the solution. X-Ray powder diffractograms revealed the identity of all isolated samples and the identity with the crystal selected for the single crystal structure determination.

Cyclic voltammetry measurements of thianthrene in liquid SO_2 were so far reported only at low temperatures ($-40\text{ }^{\circ}\text{C}$) below the boiling point of this solvent [18]. We determined the oxidation potentials

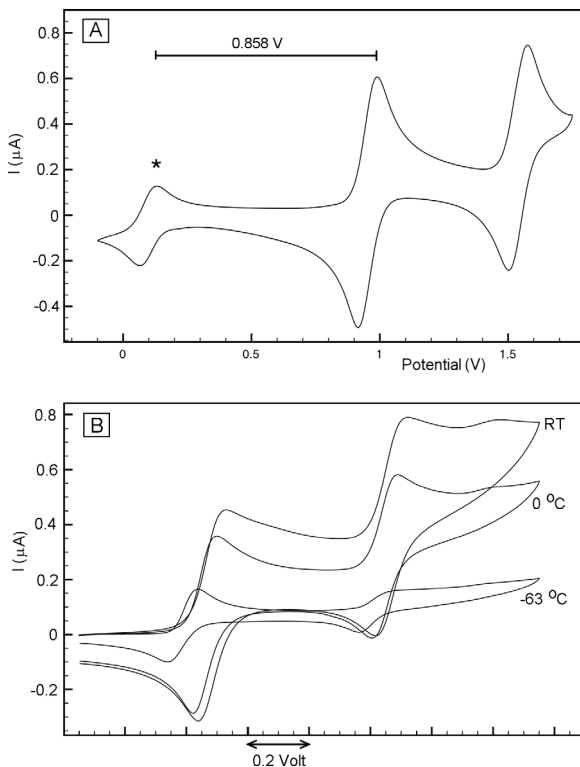


Fig. 1. Cyclic voltammetry diagrams of thianthrene in liquid SO_2 with $[NBu_4]PF_6$ as electrolyte. A: an average of 5 scans at r.t. with ferrocene (Fc) as the reference redox system (Fc/Fc^+ marked with *), B: pure thianthrene (single scans) at different temperatures.

again at ambient temperature to come close to the actual reaction conditions. Fig. 1a shows the cyclovoltamogram of TA in liquid SO_2 at $23\text{ }^{\circ}\text{C}$. Ferrocene (Fc) was used as a reference redox system [20]. The difference between the potential of the first oxidation wave of TA and Fc/Fc^+ under the applied conditions is 0.858 V. The observed potential for the first oxidation step does not differ significantly from that in acetonitrile which was measured to be 0.846 V vs. Fc/Fc^+ . On varying the temperature of the SO_2 solution from $-63\text{ }^{\circ}\text{C}$ to ambient temperature we observed a significant shift of the first oxidation wave by about 0.1 V to higher potentials (Fig. 1b). The potentials that had to be applied to oxidize TA in the respective solvents for the synthesis of the radical cation showed remarkable differences. In acetonitrile and dichloromethane a potential of 4 V between the electrodes was necessary for the occurrence of a persistent violet color of the solution and the deposition of $TA[PF_6]$ on the electrode, while in SO_2 just 2 V were sufficient. Despite

the applied high potentials in the organic solvents, no formation of the dication TA^{2+} was observed which is known as the component of tetramethylthianthrenium(2+) hexachloroantimonate [21].

$\text{TA}[\text{PF}_6]$ is highly sensitive to oxidation in solution and in the solid state and can only be handled in an argon-filled glove box. The visual melting point was 140–143 °C. In the DSC measurements, however, a broad endothermic process is observed with an onset temperature of 126 °C indicating decomposition. Different samples of $\text{TA}[\text{PF}_6]$ all showed a small endothermic process on heating to 80 °C with a heat conversion of 0.36 kJ mol⁻¹. This process seems to be irreversible since on cooling a corresponding exothermic process could not be unequivocally detected. The nature of this transition remains unknown.

Crystal structure

The crystal structure of $\text{TA}[\text{PF}_6]$ is built up of almost planar thianthrenium radical cations and of octahedral hexafluorophosphate anions. The planarity of $\text{TA}^{\bullet+}$ cations is typical for thianthrenium radical ions. The cations are bisected by mirror planes through the bonds C3–C3^I, C1–C1^I, C4–C4^I and C6–C6^I (Fig. 2). Each cation therefore has crystallographic C_s symmetry. The point group C_{2v} is, however, almost fulfilled. The two sulfur atoms and the atoms of each one of the two benzene rings form well-defined planes. The largest deviations from the best plane through S, S^I, C1, C1^I, C2, C2^I, C3, C3^I are observed for C1 and C1^I with 0.040 Å and for the plane S, S^I, C4, C4^I, C5, C5^I, C6, C6^I for C4 and C4^I with 0.034 Å. These two planes include a dihedral angle of 172.6° indicating the molecule to

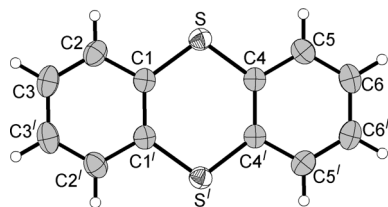


Fig. 2. The thianthrenium radical ion in the structure of $\text{TA}[\text{PF}_6]$. Displacement ellipsoids are scaled to include a probability density of 40 %. Hydrogen atoms are drawn with arbitrary radii. Selected bond lengths (Å) and angles (deg): S–C1 1.720(2), S–C4 1.719(2), C1–C2 1.398(3), C1–C1^I 1.412(4), C2–C3 1.367(3), C3–C3^I 1.398(5), C4–C5 1.403(3), C4–C4^I 1.413(4), C5–C6 1.363(3), C6–C6^I 1.400(5); C1–S–C4 107.1(1), C1^I–C1–S 126.09(7), C4^I–C4–S 126.08(7), C–C–C within aromatic rings 114.7(2) to 120.7(2). Symmetry operation: I = x, -y, z.

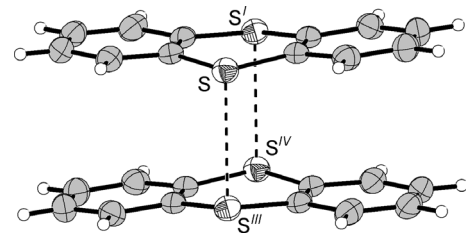


Fig. 3. A dimer of two thianthrenium radical cations in the structure of $\text{TA}[\text{PF}_6]$. Displacement ellipsoids are drawn at the 40 % probability level. The lengths of the S···S contacts between the molecules amount both to 3.066(2) Å. Symmetry operation: III = 1 – x, y, 1 – z; IV = 1 – x, –y, 1 – z.

be almost flat but slightly bent on the S···S^I axis. The respective angle in the structure of $\text{TA}[\text{AlCl}_4]$ amounts to 171.8° [14] which shows the similarity of the radical ions in both structures. The radical ions are associated to form dimers (Fig. 3). The two molecules of each pair are related by a twofold axis. Together with the mirror plane each dimer gains crystallographic C_{2h} symmetry, but is only slightly distorted from the higher symmetry point group D_{2h} . The two identical S···S intermolecular distances amount to 3.066 Å which is in between a covalent S–S bond (2.08 Å) and the van der Waals distance of two sulfur atoms (\approx 3.6 Å). The dimers are isolated from each other. The shortest S···S distances between sulfur atoms of neighboring $(\text{TA}^{\bullet+})_2$ dimers are longer (3.743 Å) than the sum of the van der Waals radii.

In $(\text{TA}^{\bullet+})[\text{AlCl}_4]^-$ the thianthrenium ions show ring slippage. Two different intermolecular S···S distances of 3.05 and 3.11 Å were found, and the S···S···S angles in the four-membered ring of sulfur atoms amount to 98° and 82° [14]. In $(\text{TA}^{\bullet+})[\text{PF}_6]^-$ the two thianthrenium radicals are in perfect overlap, and due to the local symmetry the four S···S···S angles are strictly rectangular. The interactions between molecular π -conjugated radicals can be divided into σ and π bonding [22]. For thianthrene a σ dimer is expected to exhibit a substantial bending at the intramolecular S···S axis and short intermolecular S–S bonding in the region of the length of a single bond. With almost flat molecules and quite long S···S bonds the dimers in the structure of $\text{TA}[\text{PF}_6]$ are true π dimers.

In the hexafluorophosphate anion each F atom position is split into two equally occupied positions indicating a disorder of the ion. The PF_6 octahedra have the same center of gravity within the P atom but have different orientations (Fig. 4). The P–F bond lengths

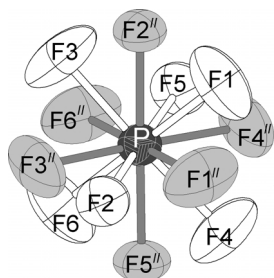


Fig. 4. The hexafluorophosphate ion in the structure of TA[PF₆]. Displacement ellipsoids are drawn to include a probability density of 40 %. The F atoms are disordered each over two positions resulting in two half occupied, superimposed [PF₆]⁻ octahedra, drawn in white and grey. Symmetry operation: II = x , 1 - y , z .

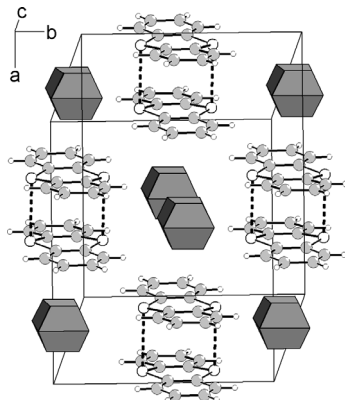


Fig. 5. The unit cell of thianthrenium hexafluorophosphate. Atoms are drawn as spheres with arbitrary radii. The disordered [PF₆]⁻ anions are represented as massive polyhedra.

are in the range from 1.559(3) to 1.603(3) Å. Each one of the two superimposed hexafluorophosphate anions is almost perfectly octahedral.

In the unit cell each radical cation dimer (TA^{•+})₂ is surrounded by twelve [PF₆]⁻ ions which are grouped into six pairs of closely neighboring anions (Fig. 5). Accordingly, each pair of [PF₆]⁻ anions has six neighboring (TA^{•+})₂ cations. The overall arrangement of the ions in the crystal structure adopts the simple rock salt type if the (TA^{•+})₂ dimers are counted as the cations and each closely neighboring pair of [PF₆]⁻ are counted as one anion. The shortest intermolecular C–H···F hydrogen bond (H3···F4, III = 0.5 + x , -0.5 + y , 1 + z) amounts to 2.435(4) Å.

Electrical conductivity

TA[PF₆] is a small-gap semiconductor. The absolute conductivity is very small at r.t. ($5 \cdot 10^{-8}$ S m⁻¹) but

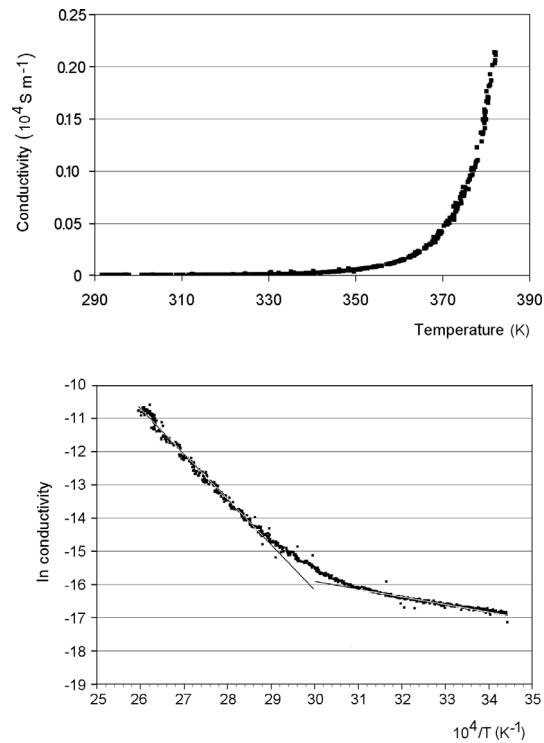


Fig. 6. The upper graph shows the electrical conductivity *vs.* temperature for a cylindrical sample of TA[PF₆] measured by the two-probe technique. In the diagram on the bottom an Arrhenius plot ln(conductivity) *vs.* reciprocal temperature is shown. There are two regions present which can each be fitted by a linear function.

readily increases with rising temperature and reaches $2.5 \cdot 10^{-5}$ S m⁻¹ at 110 °C. The temperature dependence of the conductivity is presented in Fig. 6 and can be described using the Arrhenius law $\ln \sigma = A \exp(E_a/kT)$. The function $\ln \sigma = f(T^{-1})$ in Fig. 6 shows two linear regions, a steep region between 70 and 110 °C and a flattish region between 20 and 50 °C. The overall conductivity can reasonably be described by the superposition of two thermally activated processes in an intrinsic high-temperature region with an activation energy of 1.2 eV and an extrinsic low-temperature region with low activation energy of 0.2 eV. The thermal activation energy of 1.2 eV is relatively high but can be understood considering the arrangement of the radical molecules in pairs which prevents the presence of a conducting, half-filled crystal orbital.

Band structure calculations

The electronic structure of TA[PF₆] was studied theoretically at the density-functional theory (DFT) level.

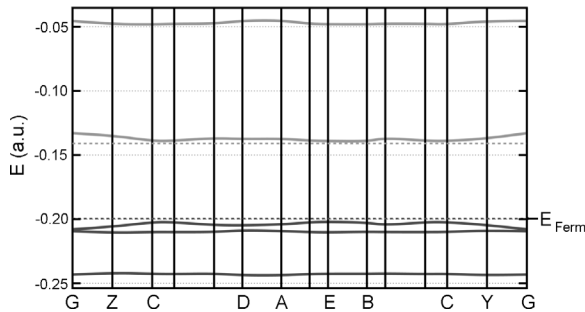


Fig. 7. Calculated band structure of the primitive TA[PF₆] unit cell in the singlet state (PW1PW, TZVP basis set); band energies are given in atomic units; 1 a. u. = 27.21 eV; the Fermi level and the bottom of the conduction band are indicated by dashed lines.

Lattice energy and band structure calculations were performed with the crystalline orbital program CRYSTAL06 [23]. Lattice parameters and atom positions were taken from the experiment and kept fixed. In CRYSTAL the Bloch functions are expanded in atom-centered basis functions. All-electron Gaussian basis sets of triple zeta valence plus polarization (TZVP) quality were used. The original TZV basis sets of Ahlrichs *et al.* [24] were slightly modified. The most diffuse *s* and *p* shells of the carbon and phosphorus atoms were removed in order to avoid linear dependencies of the basis. Polarization functions (*p* for hydrogen, *d* for phosphorus, sulfur, carbon and fluorine) were added. The hybrid exchange-correlation functional PW1PW [25] was employed. In earlier work it was shown that Hartree-Fock DFT hybrid methods give an improved account of electronic properties in oxides and other compounds compared to standard DFT methods [26]. The CRYSTAL standard values for integral accuracy were increased by a factor of ten. Integration in reciprocal space was performed using a $6 \times 6 \times 6$ Monkhorst-Pack *k*-point net (resulting in 112 points in the irreducible Brillouin zone IBZ). Both singlet and triplet states were studied for the primitive cell containing two TA^{•+} units. With PW1PW the singlet state is 0.7 eV/unit cell more stable than the triplet state, indicating strong coupling between neighboring TA radicals in the same cell. It has to be mentioned, however, that the singlet-triplet energy splitting is strongly dependent on the Hamiltonian. With the same computational setup, the Hartree-Fock method predicts the triplet state to be more stable by 0.4 eV, and a standard GGA (generalized gradient approximation) functional such as PBE [27] favors the singlet state by 1 eV. As it is well known that open-shell

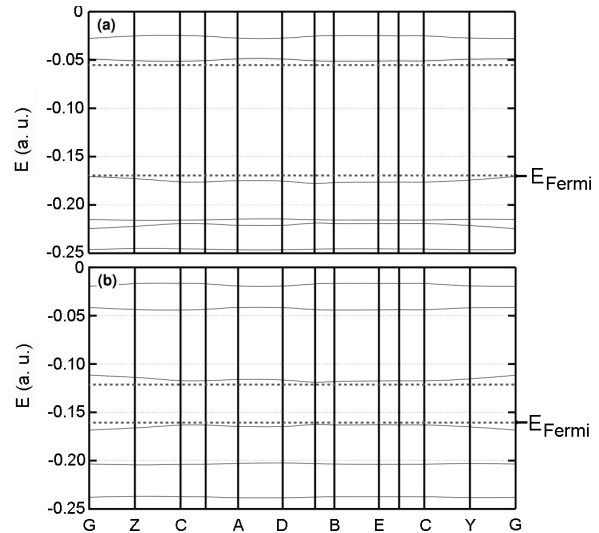


Fig. 8. Calculated band structure of the primitive TA[PF₆] unit cell in the triplet state (PW1PW, TZVP basis set); (a) α -electrons, (b) β -electrons.

systems are overly stabilized at the Hartree-Fock level whereas GGA DFT methods have a bias towards spin pairing, hybrid methods such as PW1PW are probably a reasonable compromise. A rigorous treatment at multireference *ab initio* level is required to tackle the question of the correct ground state of this system. This is beyond the scope of the present study.

Therefore in the following we discuss the calculated band structures of both multiplicities as shown in Figs. 7 and 8. Irrespective of multiplicity and spin, all bands have a rather small dispersion, indicating weak interaction between TA dimers in different unit cells. For the singlet state (Fig. 7) the maximum of the valence band (VB) and the minimum of the conduction band (CB) coincide at the C point of the IBZ ($\langle 0, 1/2, 1/2 \rangle$ in the conventional setting). The direct C–C interband transition energy is 1.5 eV. This would classify TA[PF₆] as a small-gap semiconductor.

For the majority spin component (denoted as α) of the triplet state (Fig. 8) the maximum of the valence band is at the Γ point (indicated as G) while the minimum of the conduction band is at the C point, similar as in the singlet state. The difference between minimal indirect (Γ -C) and direct (Γ - Γ) transition is, however, rather small. The α band gap is 3.2 eV. The valence band maximum and the conduction band minimum of the minority spin component (β) are both at the B point ($\langle 1/2, 0, 1/2 \rangle$). Here, the calculated band gap is much smaller than for the majority component, 0.9 eV.

Conclusion

Thianthrene (TA) can be oxidized electrochemically to the persistent radical cation $\text{TA}^{\bullet+}$ and isolated in crystalline form as the hexafluorophosphate salt by using $[\text{NBu}_4]\text{[PF}_6]$ as the electrolyte. The formation of $\text{TA}[\text{PF}_6]$ is independent of the solvent used, either CH_3CN , CH_2Cl_2 , or liquid SO_2 . The salt is stable up to 120 °C and shows electrical semiconduction with a thermal activation energy of 1.2 eV in the intrinsic high-temperature region above 70 °C. The structure contains $(\text{TA}^{\bullet+})_2 \pi$ dimers with two of the planar molecules stacked coincidentally in a dimer with two weak $S \cdots S$ bonds of 3.06 Å. These dimers are isolated in the crystal and separated by the anions which explains the semiconductivity. Theoretical calculations at hybrid density-functional level predict that $\text{TA}[\text{PF}_6]$ has a small band gap of 1.5 eV in the singlet ground state and of 0.9 eV in the excited triplet state, respectively. Both values are consistent with the observed conductivity.

Experimental Section

Thianthrene (Aldrich) was purified by recrystallization from ethanol/toluene before use. Tetrabutylammonium tetrafluoroborate (Aldrich) was used as obtained and stored over P_4O_{10} before use. All solvents were dried (CH_2Cl_2 , CH_3CN , SO_2 : P_4O_{10} ; $\text{C}_2\text{H}_5\text{OC}_2\text{H}_5$: Na) and freshly distilled prior to use.

H-shaped, two compartment glass vessels equipped with Teflon screw cocks (Young) and a glass frit between the two tubes were used [28]. A 2.8 mm hole was drilled through the axes of the Teflon cocks and a stainless steel stick (3 mm diameter) was inserted through the cocks axis. This assembly turned out to be gas-tight against the equilibrium pressure of liquid SO_2 at ambient temperature. At the end of the sticks, platinum wires were fixed to serve as electrodes. Each compartment of this electrochemical cell had a volume of about 20 mL. In the experiments a total of 100 mg thianthrene and 400 mg $[\text{NBu}_4]\text{[PF}_6]$ were placed in two equal portions in the two compartments, and about 2×20 mL solvent were filled into the cell until the liquid level reached half the height of the connecting frit.

DSC measurements were performed on 2 mg samples of $\text{TA}[\text{PF}_6]$ with a type 204 F1 Phoenix (Netzsch) scanning calorimeter. X-Ray powder diffractograms were recorded with a Stoe Stadi P diffractometer equipped with $\text{CoK}\alpha$ radiation. Conductivity measurements were performed on pressed pellets (diameter 2 mm, thickness 0.6 mm) by the two-probe technique. The pellet was inside a quartz tube clamped by two steel pistons. Heating was performed by an electrical tube oven starting from ambient temperature up to

Table 1. Crystal structure data for $\text{TA}[\text{PF}_6]$.

Formula	$\text{C}_{12}\text{H}_8\text{F}_6\text{PS}_2$
M_r	361.29
Crystal size, mm ³	$0.07 \times 0.09 \times 0.10$
Crystal system	monoclinic
Space group	$C2/m$
$a, \text{\AA}$	12.4345(8)
$b, \text{\AA}$	10.5318(6)
$c, \text{\AA}$	11.1303(7)
β, deg	112.565(3)
$V, \text{\AA}^3$	1346.0(1)
Z	4
$D_{\text{calcd.}}, \text{g cm}^{-3}$	1.78
$\mu(\text{MoK}\alpha), \text{cm}^{-1}$	5.7
$F(000), \text{e}$	724
hkl range	$\pm 16, \pm 13, \pm 14$
$((\sin \theta)/\lambda)_{\text{max}}, \text{\AA}^{-1}$	0.655
Refl. measured	13461
Refl. unique	1632
R_{int}	0.082
Parameters refined	124
$R(F) / wR(F^2)$ (all refls.)	0.042/0.102
$\text{GoF}(F^2)$	0.96
$\Delta\rho_{\text{fin}} (\text{max/min}), \text{e \AA}^{-3}$	0.48/-0.31

110 °C with 40 °C h⁻¹ and back to ambient temperature with the same temperature gradient. During the measurement the polarity of the applied direct current was frequently reversed, and all measurements were carried out twice applying a constant voltage of 1 and of 5 V.

Cyclic voltammetry measurements in liquid SO_2 at ambient temperature were performed using a Metrohm μ Autolab III analyzer in a gas- and pressure-tight glass vessel. Working and counter electrodes were made of Pt (1.65 mm² surface area), the quasi-reference electrode was a home made Pt/polypyrrole electrode [29], and $[\text{NBu}_4]\text{[PF}_6]$ was used as electrolyte. Thianthrene (5 mg, 0.023 mmol) and $[\text{NBu}_4]\text{[PF}_6]$ (968.6 mg, 2.5 mmol) were dissolved in 10 mL of liquid SO_2 ; ferrocene (4.7 mg, 0.025 mmol) was used as reference redox system. The applied scan rate was 0.2 V s⁻¹.

Preparation of $\text{TA}[\text{PF}_6]$ in CH_2Cl_2

A constant voltage of 4 V was applied during four days at ambient temperature. The anode was slowly covered with a polycrystalline film of $\text{TA}[\text{PF}_6]$. The electrode was removed from the solution, and the layer of $\text{TA}[\text{PF}_6]$ was mechanically removed from the electrode in an argon-filled glove box.

Preparation of $\text{TA}[\text{PF}_6]$ in CH_3CN

A constant voltage of 4 V was applied during three days at ambient temperature. The anodic compartment gained a dark blue color while the cathodic solution turned amber. Under a flow of argon, the cell was opened and the anolyte transferred to a Schlenk tube. The volume of the solution was reduced to

1/3 by distilling off the solvent. The original amount of solvent volume was restored by layering the concentrated acetonitrile solution with diethyl ether. Slow diffusion of Et₂O into the CH₃CN solution while storing at –18 °C caused the precipitation of bronze-colored crystals which were filtered off under argon. Yield: 108 mg (31.5 % of theory).

Preparation of TA[PF₆] in liquid SO₂

About 40 mL of liquid SO₂ was condensed into the cell loaded with TA and [NBu₄][PF₆]. A constant voltage of 2 V was applied leading to a current of 0.2 mA. The anolyte turned dark blue and the catholyte dark red. By slowly releasing gaseous SO₂ after three days at r.t., the solutions were concentrated to one third of the original volume. Storing at –18 °C for two days afforded a precipitation of dark crystals in the anodic compartment. The supernatant solution was filtered into the second compartment of the closed and cold cell. The SO₂ vapor was released, and 120 mg (35 % of theory) of black, bronze-shining crystals were isolated. — Analysis for C₁₂H₈F₆PS₂: calcd. C 39.89, H 2.23, S 17.75; found C 39.83, H 2.09, S 17.60.

X-Ray structure determination

Crystals were selected in the glove box and fixed in capillaries which were sealed by melting. Crystals grown from

acetonitrile showed better diffraction patterns than those from liquid SO₂. Data collection was performed at ambient temperature using a Bruker-Nonius kappa-CCD diffractometer equipped with graphite-monochromatized MoK_α radiation. The crystal structure was solved by Direct Methods and refined using the SHELX97 programs [30]. A semi empirical absorption correction by the multi-scan method was applied to the data set [31]. Hydrogen atoms were refined as riding on their attached carbon atoms with isotropic displacement factors fixed to the value 1.2 of the respective C atoms. The F atom positions of the [PF₆][–] ion turned out to be disordered each over two positions and were refined on split positions with occupation factors fixed to 0.5. Crystal data and details of the structure determinations are summarized in Table 1.

CCDC 701449 contains the supplementary crystallographic data for this paper. These data can be obtained free of charge from The Cambridge Crystallographic Data Centre via www.ccdc.cam.ac.uk/data_request/cif.

Acknowledgements

The support of this work by the German Research Council (DFG) within the Collaborative Research Area SFB 813 is gratefully acknowledged. We thank Dr. J. Daniels for the collection of X-ray diffraction data, N. Wagner for his efforts with the conductivity measurements and S. von Erichsen for assistance in the synthetic work.

-
- [1] G. Stenhouse, *Proc. Royal Soc. London* **1868**, *17*, 62–72.
 - [2] K. L. Gallaher, S. H. Bauer, *J. Chem. Soc., Faraday Trans. 2*, **1975**, *71*, 1173–1182.
 - [3] S. B. Larson, S. H. Simonsen, G. E. Martin, K. Smith, S. Puig-Torres, *Acta Crystallogr.* **1984**, *C40*, 103–106.
 - [4] M. E. Amato, A. Grassi, K. J. Irgolic, G. C. Pappalardo, L. Radics, *Organometallics* **1993**, *12*, 775–780.
 - [5] V. S. Mastryukukov, K.-H. Chen, S. H. Simonsen, N. L. Albinger, J. E. Boggs, *J. Mol. Struct.* **1997**, *413–414*, 1–12.
 - [6] A. Ito, H. Ino, H. Ichiki, K. Tanaka, *J. Phys. Chem. A* **2002**, *106*, 8716–8720.
 - [7] S. Kim, Y. Kwon, J.-P. Lee, S.-Y. Choi, J. Choo, *J. Mol. Struct.* **2003**, *655*, 451–458.
 - [8] J. V. de Vondele, R. Lyriden-Bell, E. J. Meyer, M. Sprik, *J. Phys. Chem. B* **2006**, *110*, 3614–3623.
 - [9] E. A. C. Lucken, *J. Chem. Soc.* **1962**, 4963–4965.
 - [10] W. Rundel, L. Scheffler, *Tetrahedron Lett.* **1963**, 993–995.
 - [11] Y. Murata, L. Hughes, H. J. Shine, *Inorg. Nucl. Chem. Lett.* **1968**, *4*, 573–576.
 - [12] Y. Sato, M. Kinoshita, M. Sano, H. Akamatu, *Bull. Chem. Soc. Jpn.* **1967**, *40*, 2539–2542.
 - [13] B. K. Bandlish, H. J. Shine, *J. Org. Chem.* **1977**, *42*, 561–563.
 - [14] H. Bock, A. Rauschenbach, Ch. Näther, M. Kleine, Z. Havlas, *Chem. Ber.* **1994**, *127*, 2043–2049.
 - [15] M. de Sorgo, B. Wassermann, M. Szwarc, *J. Phys. Chem.* **1972**, *76*, 3468–3471.
 - [16] P. Rapta, L. Kress, P. Hapiot, L. Dunsch, *Phys. Chem. Chem. Phys.* **2002**, *4*, 4181–4185.
 - [17] S. V. Rosokha, J. Lu, T. J. Rosokha, J. K. Kochi, *Acta Crystallogr.* **2007**, *C63*, o347–o349.
 - [18] L. A. Tinker, A. J. Bard, *J. Am. Chem. Soc.* **1979**, *101*, 2316–2319.
 - [19] O. Hammerich, V. D. Parker, *Electrochim. Acta* **1973**, *18*, 537–541.
 - [20] G. Gritzner, J. Kuta, *Pure & Applied Chem.* **1984**, *56*, 461–466.
 - [21] H. Bock, A. Rauschenbach, K. Ruppert, Z. Havlas, *Angew. Chem.* **1991**, *103*, 706–708; *Angew. Chem., Int. Ed. Engl.* **1991**, *30*, 714–716.
 - [22] T. Nishinaga, K. Komatsu, *Org. Biomol. Chem.* **2005**, *3*, 561–569.
 - [23] R. Dovesi, V. R. Saunders, C. Roetti, R. Orlando, C. M. Zicovich-Wilson, F. Pascale, B. Civalleri, K. Doll, N. M. Harrison, I. J. Bush, Ph. D'Arco, M. Llunell,

- CRYSTAL06, User's Manual, University of Torino, Torino (Italy) **2006**.
- [24] A. Schäfer, C. Huber, R. Ahlrichs, *J. Chem. Phys.* **1994**, *100*, 5829–5835.
- [25] T. Bredow, A. R. Gerson, *Phys. Rev. B* **2000**, *61*, 5194–5201.
- [26] F. Cora, M. Alfredsson, G. Mallia, D. S. Middlemiss, W. C. Mackrodt, R. Dovesi, R. Orlando, *Struct. Bond.* **2004**, *113*, 171–232.
- [27] J. P. Perdew, K. Burke, M. Ernzerhof, *Phys. Rev. Lett.* **1996**, *77*, 3865–3868.
- [28] J. Beck, F. Steden, *Z. Naturforsch.* **2003**, *58b*, 711–714.
- [29] J. Ghilane, P. Haplot, A. J. Bard, *Anal. Chem.* **2006**, *78*, 6868–6872.
- [30] G. M. Sheldrick, SHELXS/L-97 (release 97-2), Programs for Crystal Structure Determination, University of Göttingen, Göttingen (Germany) **1997**.
- [31] R. H. Blessing, *Acta Crystallogr.* **1995**, *A51*, 33–38.